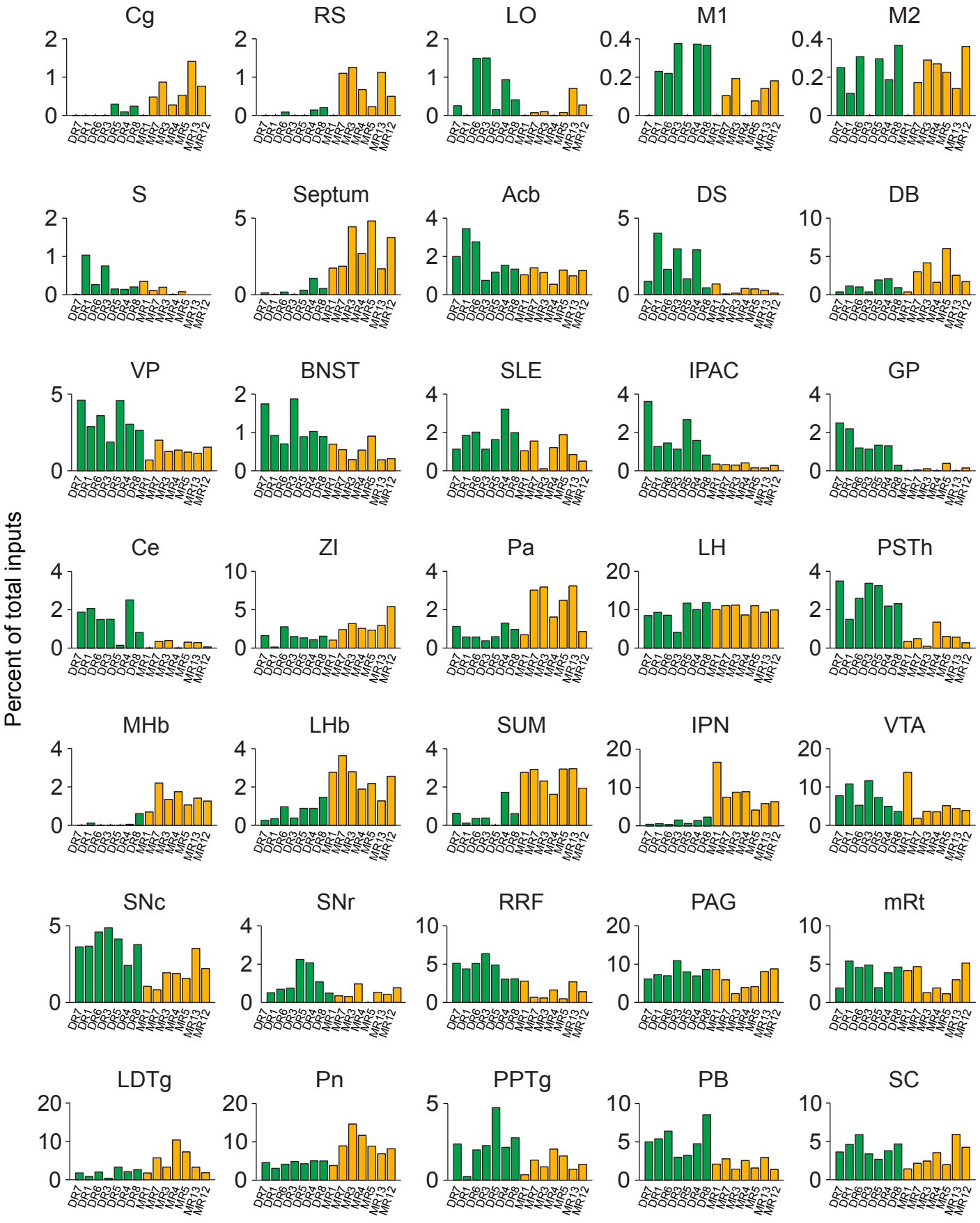
Percent of total inputs
Cg
RS
LO
M1
M2
S
Septum
Acb
DS
DB
VP
BNST
SLE
IPAC
GP
Ce
ZI
Pa
LH
PSTh
MHb
LHb
SUM
IPN
VTA
SNc
SNr
RRF
PAG
mRt
LDTg
Pn
PPTg
PB
SC
DR7 DR1 DR6 DR3 DR5 DR4 DR8 MR1 MR7 MR3 MR4 MR5 MR13 MR12

Figure S1. Percent of total inputs from individual animals (Related to Figure 1)

Cg, cingulate cortex; RS, retrosplenial granular cortex; LO, lateral orbital cortex; M1, primary motor cortex; M2, secondary motor cortex; S, somatosensory cortex; Septal nucleus; Acb, nucleus accumbens; DS, dorsal striatum; DB diagonal band of broca; VP, vental pallidum; BNST, bed nucleus of the stria terminalis; SLE, sublenticular extended amygdala; IPAC, interstitial nucleus of the posterior limb of the anterior commissure; GP, globus pallidus; Ce, central nucleus of the amygdala; ZI, zona incerta; Pa, paraventricular hypothalamic nucleus; LH, lateral hypothalamic area; PSTh, parasubthalamic nucleus; MHb, medial habenula; LHb, lateral habenula; SUM, supramammillary nucleus; IPN, interpeduncular nucleus; VTA, ventral tegmental area; SNc, substantia nigra pars compacta; SNr, substantia nigra pars reticulate; RRF, retrorubral field; PAG, periaqueductal gray; mRt, mesencephalic reticular formation; LDTg, laterodorsal tegmental nucleus; Pn, pontine reticular nucleus; PPTg, pedunculotegmental nucleus ; PB, parabrachial nucleus; SC, superior colliculus.

A

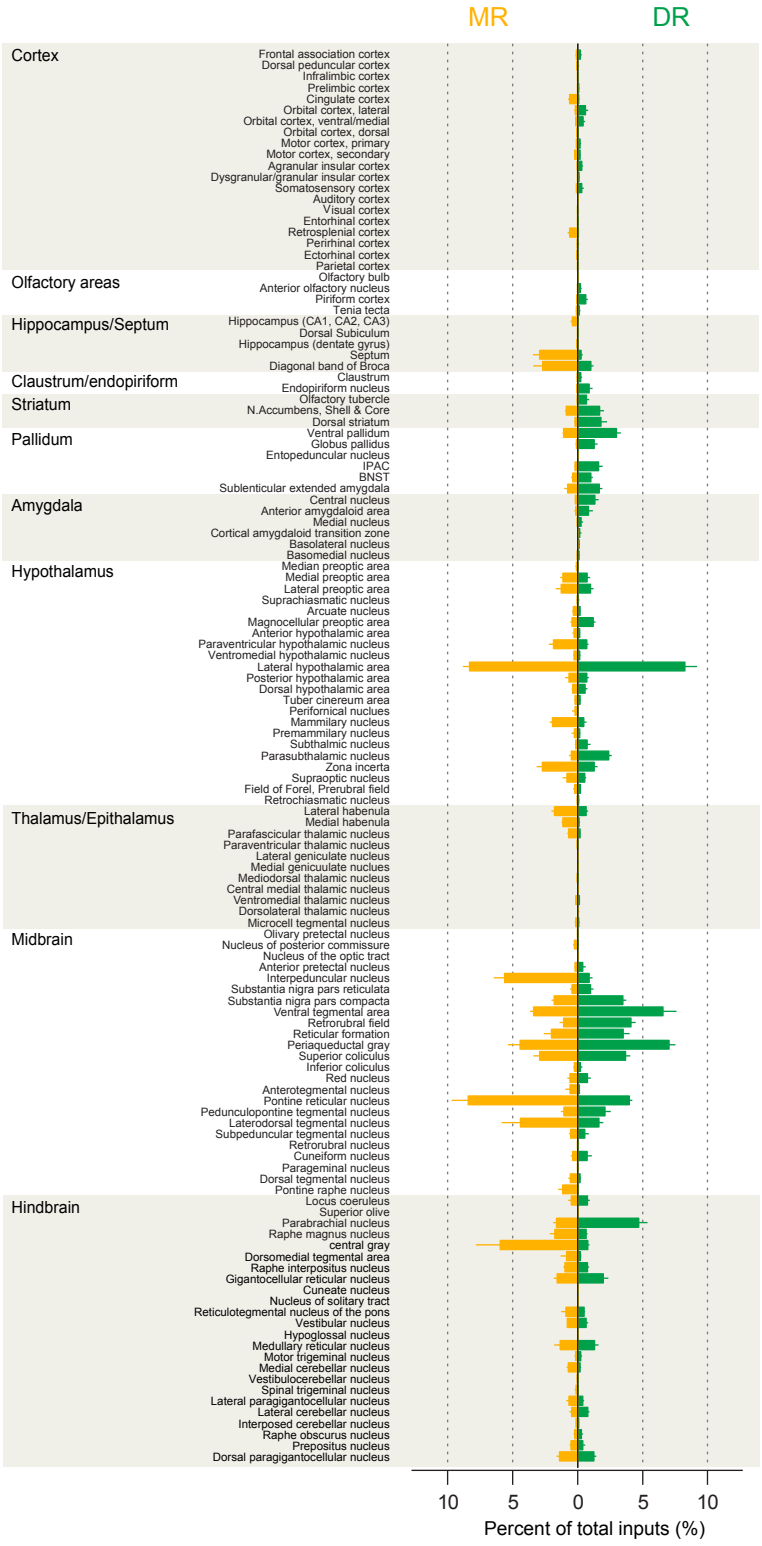
MR
DR
Cortex
Frontal association cortex
Dorsal peduncular cortex
Infralimbic cortex
Prelimbic cortex
Cingulate cortex
Orbital cortex, lateral
Orbital cortex, ventral/medial
Orbital cortex, dorsal
Motor cortex, primary
Motor cortex, secondary
Agranular insular cortex
Dysgranular/granular insular cortex
Somatosensory cortex
Auditory cortex
Visual cortex
Entorhinal cortex
Retrosplenial cortex
Perirhinal cortex
Ectorhinal cortex
Parietal cortex
Olfactory areas
Olfactory bulb
Anterior olfactory nucleus
Piriform cortex
Tenia tecta
Hippocampus/Septum
Hippocampus (CA1, CA2, CA3)
Dorsal Subiculum
Hippocampus (dentate gyrus)
Septum
Diagonal band of Broca
Claustrum/endopiriform
Claustrum
Endopiriform nucleus
Striatum
Olfactory tubercle
N.Accumbens, Shell & Core
Dorsal striatum
Pallidum
Ventral pallidum
Globus pallidus
Entopeduncular nucleus
IPAC
BNST
Sublenticular extended amygdala
Amygdala
Central nucleus
Anterior amygdaloid area
Medial nucleus
Cortical amygdaloid transition zone
Basolateral nucleus
Basomedial nucleus
Hypothalamus
Median preoptic area
Medial preoptic area
Lateral preoptic area
Suprachiasmatic nucleus
Arcuate nucleus
Magnocellular preoptic area
Anterior hypothalamic area
Paraventricular hypothalamic nucleus
Ventromedial hypothalamic nucleus
Lateral hypothalamic area
Posterior hypothalamic area
Dorsal hypothalamic area
Tuber cinereum area
Perifornical nucleus
Mammilary nucleus
Premammilary nucleus
Subthalmic nucleus
Parasubthalamic nucleus
Zona incerta
Supraoptic nucleus
Field of Forel, Prerubral field
Retrochiasmatic nucleus
Thalamus/Epithalamus
Lateral habenula
Medial habenula
Parafascicular thalamic nucleus
Paraventricular thalamic nucleus
Lateral geniculate nucleus
Medial geniculate nucleus
Mediodorsal thalamic nucleus
Central medial thalamic nucleus
Ventromedial thalamic nucleus
Dorsolateral thalamic nucleus
Microcell tegmental nucleus
Midbrain
Olivary pretectal nucleus
Nucleus of posterior commissure
Nucleus of the optic tract
Anterior pretectal nucleus
Interpeduncular nucleus
Substantia nigra pars reticulata
Substantia nigra pars compacta
Ventral tegmental area
Retrorubral field
Reticular formation
Periaqueductal gray
Superior coliculus
Inferior coliculus
Red nucleus
Anterotegmental nucleus
Pontine reticular nucleus
Pedunculopontine tegmental nucleus
Laterodorsal tegmental nucleus
Subpeduncular tegmental nucleus
Retrorubral nucleus
Cuneiform nucleus
Parageminal nucleus
Dorsal tegmental nucleus
Pontine raphe nucleus
Hindbrain
Locus coeruleus
Superior olive
Parabrachial nucleus
Raphe magnus nucleus
central gray
Dorsomedial tegmental area
Raphe interpositus nucleus
Gigantocellular reticular nucleus
Cuneate nucleus
Nucleus of solitary tract
Reticulotegmental nucleus of the pons
Vestibular nucleus
Hypoglossal nucleus
Medullary reticular nucleus
Motor trigeminal nucleus
Medial cerebellar nucleus
Vestibulocerebellar nucleus
Spinal trigeminal nucleus
Lateral paragigantocellular nucleus
Lateral cerebellar nucleus
Interposed cerebellar nucleus
Raphe obscurus nucleus
Prepositus nucleus
Dorsal paragigantocellular nucleus
10
5
0
5
10
Percent of total inputs (%)

B

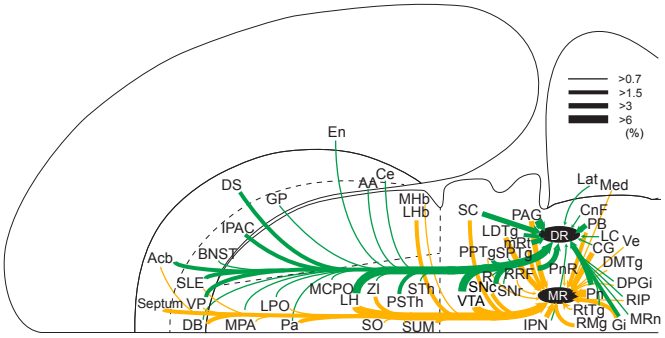
>0.7
>1.5
>3
>6
(%)
En
Ce
AA
DS
GP
MHb
LHb
SC
PAG
Lat
Med
CnF
PB
LC
Ve
CG
DMTg
DR
LDTg
RtTg
PPTg
SPTg
PnR
RRF
SNc
SNr
VTA
MR
Pn
DPGi
RIP
MRn
RtTg
RMg
Gi
IPN
1PAC
BNST
Acb
SLE
Septum
VP
LPO
MCPO
LH
ZI
STh
PSTh
SO
SUM
DB
MPA
Pa

Figure S2. Summary of monosynaptic inputs to DR and MR serotonin neurons including caudal hindbrain areas (Related to Figure 2)

(A) Monosynaptic inputs to MR and DR serotonin neurons including caudal hindbrain areas (orange and green, respectively). The values are the percentages of total inputs in each area. Twenty areas of caudal hindbrain are added to Figure 2, and the percentages of total inputs in each area are recalculated based on all brain areas. Mean ± SEM (n = 7 and 5 mice for DR and MR groups, respectively). DR and MR areas are excluded from the analysis.

(B) Flatmap summary of monosynaptic inputs to DR and MR serotonin neurons. Green indicates inputs to DR serotonin neurons. Orange indicates inputs to MR serotonin neurons. The thickness of each line indicates the percentage of total inputs in each area as defined at the top right corner. The flatmap representation is after Swanson (2000).

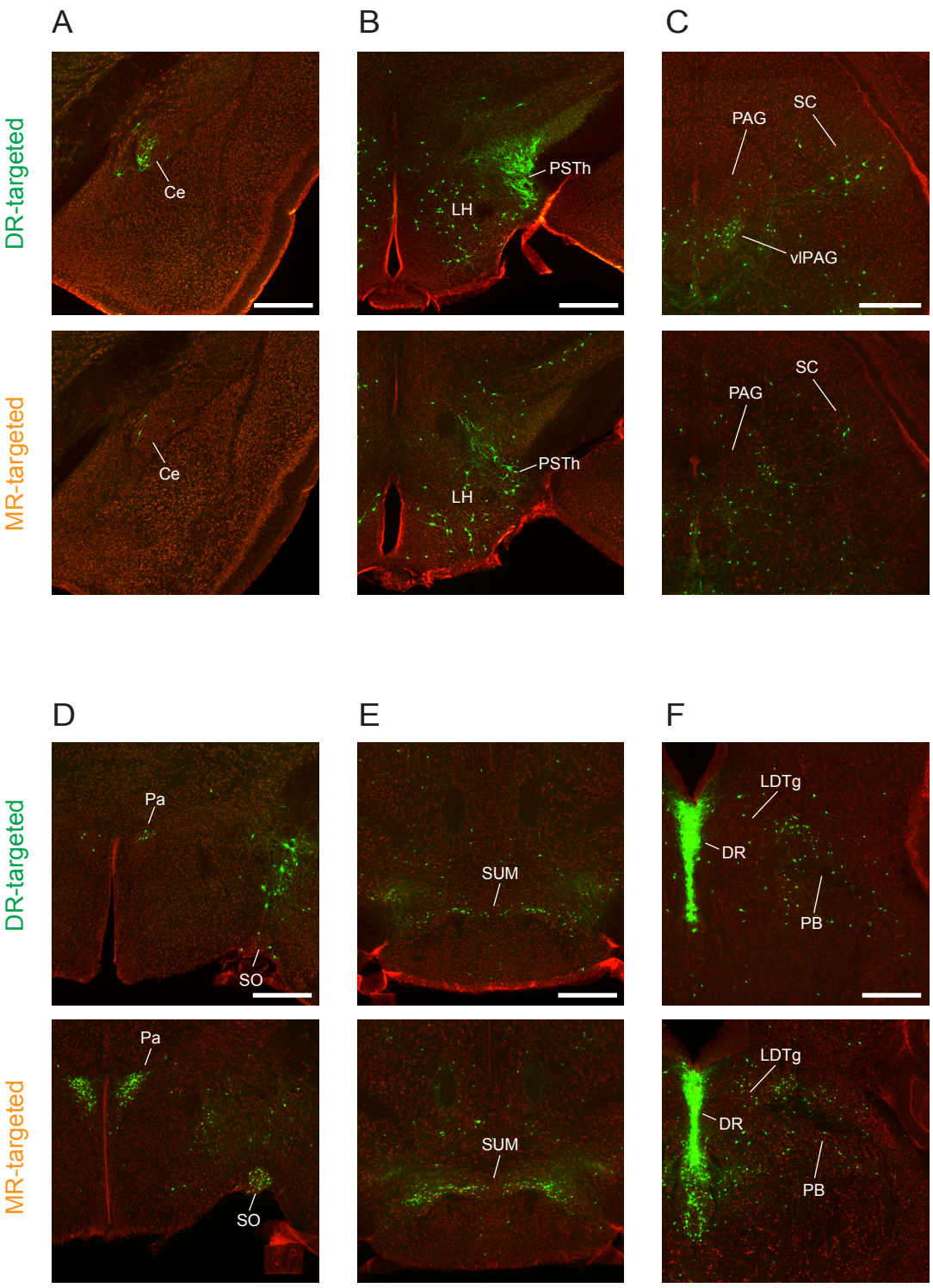
A
B
C
DR-targeted
MR-targeted
Ce
PSTh
LH
PAG
SC
vlPAG
D
E
F
Pa
SO
SUM
LDTg
DR
PB

Figure S3. Comparisons of other major input areas (Related to Figure 3)

(A) Central nucleus of the amygdala (Ce). Ce projects to DR more than MR serotonin neurons. Bregma –1.70 mm. Scale bars, 0.5 mm.

(B) Lateral hypothalamic area (LH) and parasubthalamic nucleus (PSTh). Serotonin-projecting neurons in LH are sparsely distributed. PSTh neurons project to DR more than MR serotonin neurons. Bregma –2.30 mm. Scale bars, 0.5 mm.

(C) PAG, periaqueductal gray and SC, superior colliculus. DR serotonin-projecting neurons are clustered in the ventrolateral part of the PAG (vlPAG) and ventral part of SC, whereas MR serotonin-projecting neurons are sparsely distributed in these areas. Bregma –4.04 mm. Scale bars, 0.5 mm.

(D) Paraventricular hypothalamic nucleus (Pa) and supraoptic nucleus (SO). Pa projects to MR more than DR serotonin neurons. Bregma –0.82 mm. Scale bars, 0.5 mm.

(E) Supramammillary nucleus (SUM). SUM projects to MR more than DR serotonin neurons. Bregma –2.70 mm. Scale bars, 0.5 mm.

(F) Laterodorsal tegmental nucleus (LDTg) and parabrachial nucleus (PB). LDTg projects to MR more than DR serotonin neurons. Bregma –4.96 mm. Scale bars, 0.5 mm.

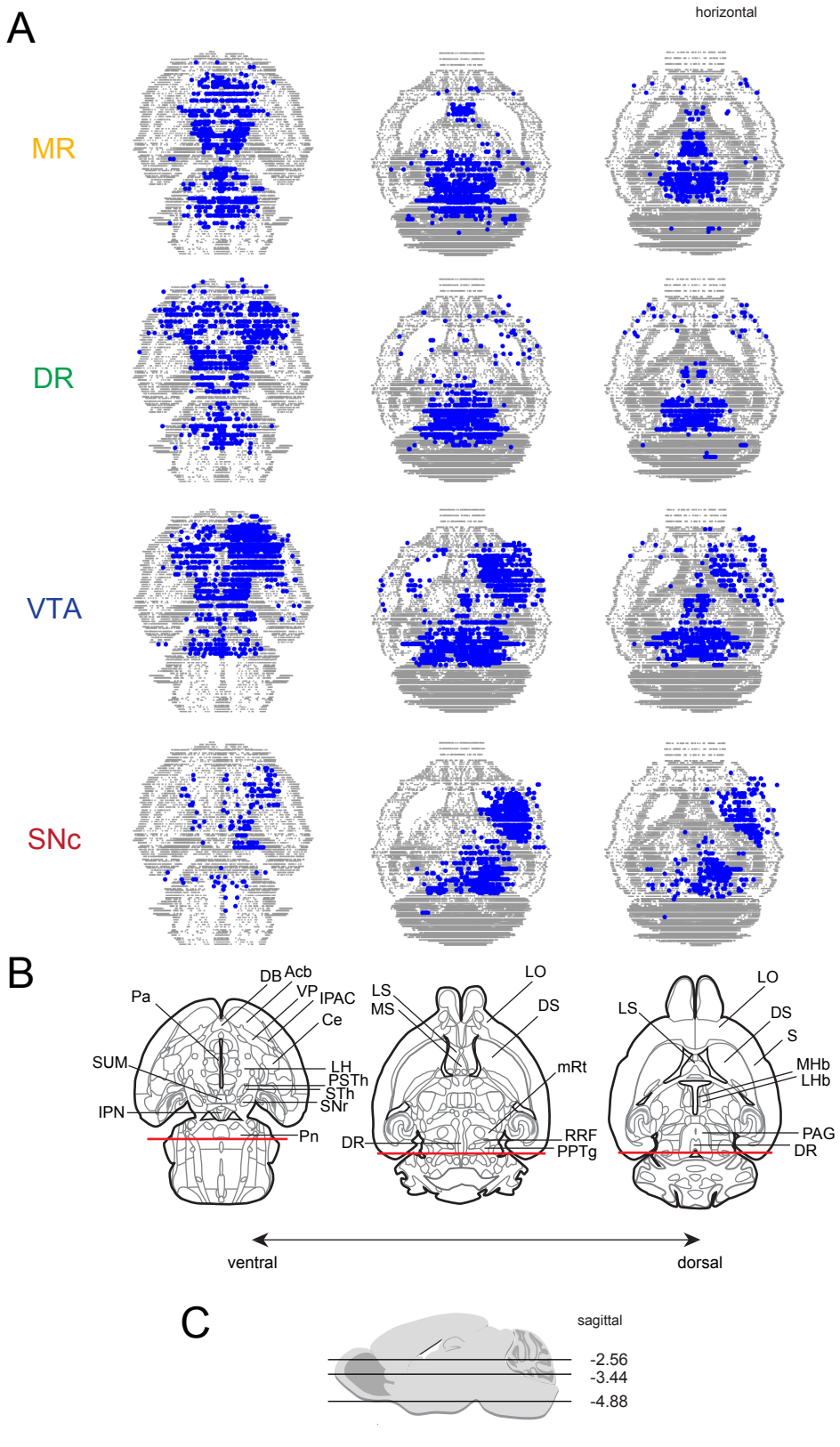
A
horizontal
MR
DR
VTA
SNc
B
DB
Acb
Pa
VP
IPAC
Ce
SUM
LH
PSTh
STh
SNr
IPN
Pn
LO
LS
MS
DS
mRt
DR
RRF
PPTg
LO
LS
DS
S
MHb
LHb
PAG
DR
ventral
dorsal
C
sagittal
-2.56
-3.44
-4.88

Figure S4. Distributions of monosynaptic inputs projected onto reconstructed horizontal slices

(A) Data obtained from coronal slices were projected onto a 3D standard brain atlas. Each image represents a horizontal slice of the standardized brain (500 μm thick). Blue dots represent input neurons from two mice each (MR; MR12 and MR13, DR; DR1 and DR6, VTA; v009 and v010, and SNc; s003 and s006). Note that the starter neurons for MR and DR are in both hemispheres while starter neurons in VTA and SNc are in one hemisphere.

(B) Atlas corresponding to each horizontal section. Input neurons were collected anterior to red lines. Bregma -5.34 mm.

(C) Approximate positions of horizontal images shown in (A) and (B).

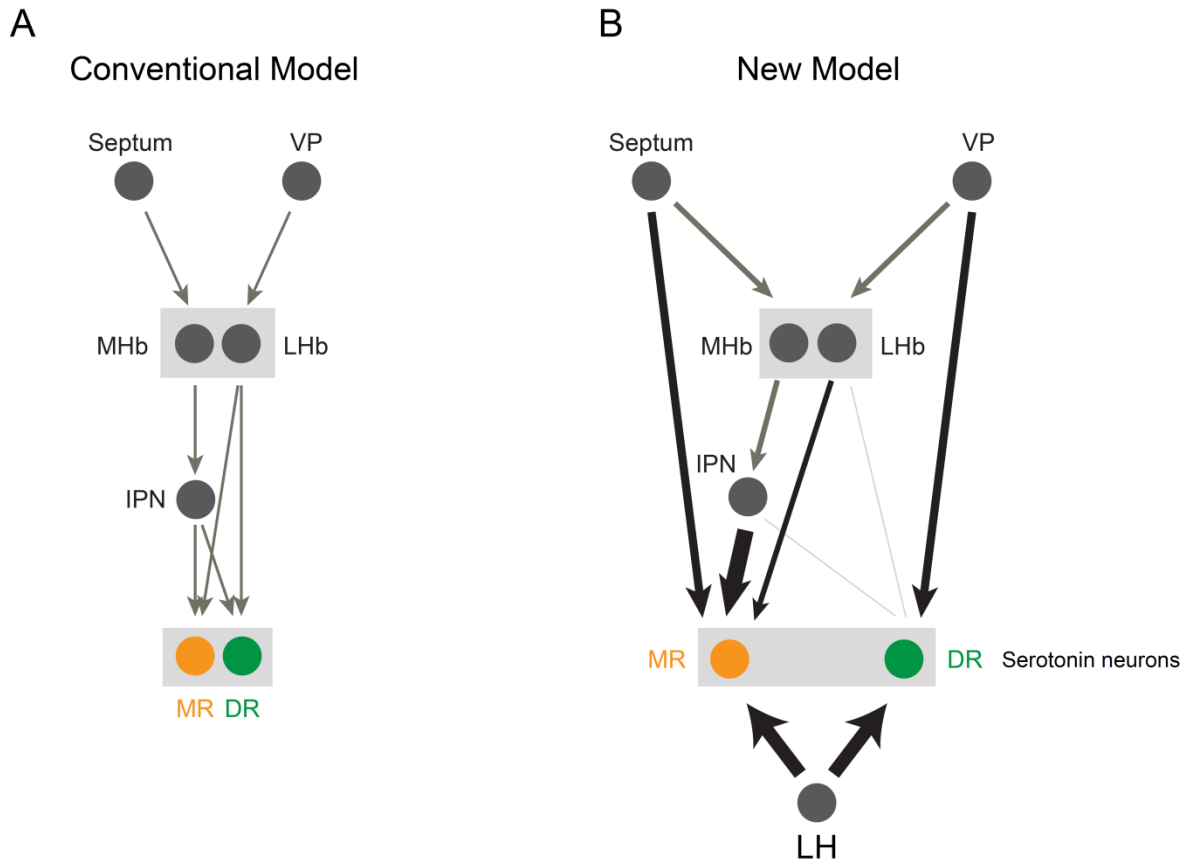

Figure S5. Models of information flow from forebrain to MR/DR serotonin neurons

(A) Conventional model. The major forebrain projections to both MR and DR, serotonin neurons are believed to come from MHb via IPN and LHb, although there are observations of projections from other areas (Herkenham and Nauta, 1979; Hikosaka et al., 2008; Klemm, 2004; Lecourtier and Kelly, 2007).

(B) New model. Whereas MR serotonin neurons receive projections from the forebrain through MHb and LHb, in addition to direct projections from the septum, DR serotonin neurons receive direct projections from the basal ganglia and the extended amygdale. LH provides the largest inputs to both MR and DR serotonin neurons. The thickness of each black arrow to serotonin neurons indicates the percentage of total inputs in each area. Light grey lines indicate small projections (less than 1 % of total inputs). Some connections are omitted for simplicity.

SUPPLEMENTAL NOTE

Previous studies found that some TVA-negative (or Cre-negative) neurons were infected nonspecifically by the rabies virus (Miyamichi et al., 2013; Wall et al., 2013; Watabe-Uchida et al., 2012). This is likely due to the extremely high infection efficiency of the rabies virus (very minute expression of TVA is sufficient for rabies infection) and due to a very low level of TVA expression that inevitably occurs in the absence of Cre (i.e., "leak" expression). However, these neurons express negligible levels of RG, a high level of which is required for transsynaptic spread of the rabies virus. Thus, these neurons are very unlikely to contribute significantly to transsynaptic labeling outside injection sites (Miyamichi et al., 2013; Wall et al., 2013; Watabe-Uchida et al., 2012). To test whether Cre-negative cells contributed as starter neurons, we performed control experiments using wild-type mice that had no Cre expression (**Figure 1A**). Consistent with a previous study (Watabe-Uchida et al, 2012), injections of the three viruses in DR resulted in a noticeable number of EGFP-positive neurons at the injection sites (29.7 ± 15.6 neurons in DR). However, a very small number of EGFP-labeled neurons were found outside injection sites (1.67 ± 0.88 neurons outside DR; mean ± SEM, n = 3 mice), many fewer than those found in experimental animals (3,577 ± 827 neurons outside DR; mean ± SEM, n = 7 mice). Thus, only a negligible number of neurons (0.05% of total input neurons) was non-specifically labeled outside the injection site. Because injection sites contained some non-specifically-labeled neurons in control animals (about 7.78% of the number of starter neurons in experimental animals), our analysis focuses on neurons outside injection sites. No mCherry-positive neurons were found outside injection sites (except in adjacent nuclei that contain serotonin neurons, as discussed above), whereas a large number of EGFP-positive neurons were found (**Figure 1G**).

SUPPLEMENTAL EXPERIMENTAL PROCEDURE

Image Analysis

To compare horizontal distributions of inputs using standardized coordinates, brains of individual animals were fit to a standard atlas (Franklin and Paxinos, 2008). The following brains were used for this analysis: DR1, DR6, MR12, MR13, v009, v010, s003, and s006. Each coronal section in the standard atlas and its matching section in our data was manually landmarked with five points: four peripheral and one central. Next, affine transformations warped the section in our data to the corresponding section in the atlas using the landmarks. We then made horizontal projections of the atlas and the data based on those points in 3-dimensional space (**Figure S4**).

SUPPLEMENTAL REFERENCES

Hikosaka, O., Sesack, S.R., Lecourtier, L., and Shepard, P.D. (2008). Habenula: crossroad between the basal ganglia and the limbic system. J. Neurosci. Off. J. Soc. Neurosci. *28*, 11825–11829.

Klemm, W.R. (2004). Habenular and interpeduncularis nuclei: shared components in multiple-function networks. Med. Sci. Monit. *10*, RA261–273.

Lecourtier, L., and Kelly, P.H. (2007). A conductor hidden in the orchestra? Role of the habenular complex in monoamine transmission and cognition. Neurosci. Biobehav. Rev. *31*, 658–672.